Hybrid free-surface flows in a two-dimensional channel

Benjamin James Binder*
University of Adelaide, Adelaide, South Australia

Jean-Marc Vanden-Broeck†
University College London, London, United Kingdom

(Received 22 February 2011; revised manuscript received 18 May 2011; published 11 July 2011)

Hybrid free-surface flows past disturbances in a two-dimensional channel are identified and studied. The fluid is assumed to be inviscid and incompressible, and the flow to be steady and irrotational. The disturbances consist of a step in the bottom of the channel and a flat object lying on the free-surface (e.g., a sluice gate). A weakly nonlinear one-dimensional analysis is used to classify the possible types of solutions, and nonlinear solutions are obtained numerically by a boundary integral equation method.

DOI: 10.1103/PhysRevE.84.016302 PACS number(s): 47.90.+a

I. INTRODUCTION

There is extensive literature on free-surface flows past disturbances in an open channel. Steady, unsteady, two-dimensional, and three-dimensional flows have been investigated [1–32]. Here we restrict our attention to two-dimensional steady potential flows. There are four basic types of disturbances: a submerged obstacle on the bottom of the channel [1–5], a step in the bottom of the channel [6–9], an object lying on the free surface [10–17], or a distribution of pressure [19–24] acting on the free surface.

When there is only one disturbance in the channel, the solutions are qualitatively independent of the type of disturbance. The solutions can then be classified as supercritical flows, subcritical flows, hydraulic falls, and generalized critical flows. All these flows exist for submerged obstacles, steps, and pressure distributions. For objects of arbitrary shape lying on the free surface (e.g., sluice gates), there are supercritical and generalized critical flows [16]. Hydraulic falls and subcritical flows are also possible, but only when there are some restrictions on the shape of the sluice gate [17]. Physical interpretations of hydraulic falls (with or without trapped waves) were also studied by Ee *et al*. [18], who considered flow over a hole or trench in the channel bottom topography.

When there is more than one disturbance, more complicated solutions are possible. We shall refer to these extra solutions as hybrid solutions. Hybrid solutions are found to depend on the type of disturbances used. They were studied for two submerged obstacles [25,26] and a sluice gate combined with a pressure distribution or a submerged obstacle [27].

Here we consider another configuration with two disturbances, namely, that of a sluice gate and a step in the bottom of the channel (see Fig. 1).

Two mathematical approaches are used. The first is a weakly nonlinear analysis based on long wave asymptotics. This weakly nonlinear approach enables a classification of all the possible solutions. The second is a boundary integral equation method which is used to compute fully nonlinear solutions. The weakly nonlinear solutions are found to be in good agreement with the fully nonlinear solutions over a large range of values of the parameters.

II. FORMULATION

Consider the steady two-dimensional irrotational flow of an incompressible inviscid fluid past a flat sluice gate (separating two free surfaces) of length L^*, and a step of height h^*, in the bottom of a channel (see Fig. 1). The sluice gate is inclined at an angle $0 < \sigma_c < \pi/2$ to the horizontal. The fluid flows from left to right, and Cartesian coordinates (x^*, y^*) are defined with the y^* axis ($x^* = 0$) passing through the point where the upstream free surface separates (tangentially) from the sluice gate. The downstream free surface separates (tangentially) from the sluice gate at $x^* = x_c^*$. The bottom of the channel is denoted by $y^* = \sigma^*(x^*)$, with the position of the step at $x^* = x_h^*$.

The equation of the free surfaces can be written as $y^* = H + \eta^*(x^*)$, where the free-surface elevation $\eta^*(x^*)$ is assumed to vanish as $x^* \to \infty$, with the flow approaching a uniform stream of constant velocity U and constant depth H. The downstream Froude number can then be defined as

$$F = \frac{U}{(gH)^{1/2}}, \tag{1}$$

where g is the acceleration due to gravity. The flow as $x^* \to -\infty$ can either approach a uniform stream with constant velocity V and constant depth $D - h^*$, or possess a train of waves. When the flow is uniform as $x^* \to -\infty$, we define an additional Froude number,

$$F^* = \frac{V}{[g(D - h^*)^{1/2}]}. \tag{2}$$

The dynamic boundary condition on the free surfaces AB and CD gives

$$\tfrac{1}{2}(u^{*2} + v^{*2}) + g\eta^*(x^*) = \tfrac{1}{2}U^2 \quad \text{on} \quad y^* = H + \eta^*(x^*), \tag{3}$$

where u^* and v^* are the horizontal and vertical components of the velocity. Here, we have used the conditions $u^* \to U$, $v^* \to 0$, $\eta^*(x^*) \to 0$ as $x^* \to \infty$, in order to evaluate the Bernoulli constant on the right-hand side of Eq. (3).

*benjamin.binder@adelaide.edu.au
†broeck@math.ucl.ac.uk

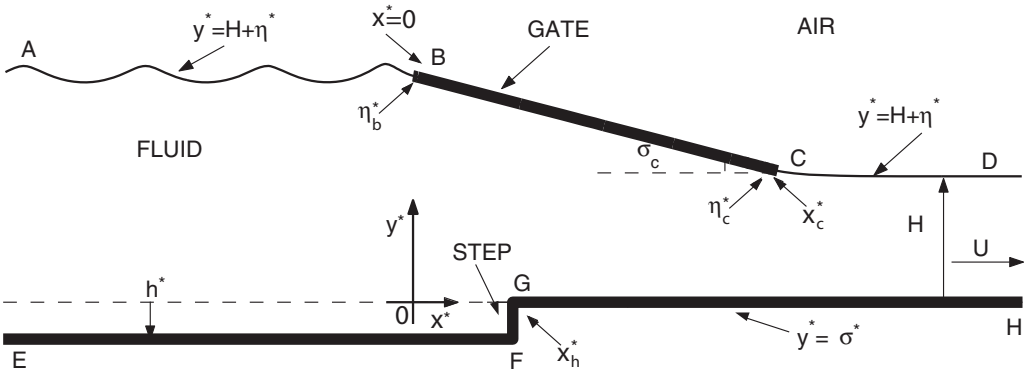

FIG. 1. Sketch of the flow configuration.

In previous work we considered separately, flows past a sluice gate [16] and flows past a step [8]. Here we investigate a configuration in which there are both a sluice gate and a step (see Fig. 1). We shall concentrate on different solutions that are not simple matchings of the already found solutions in [16] and [8]. We refer to these solutions as hybrid solutions. As is usual for flows under a sluice gate, we restrict our attention to flows with $F \geqslant 1$. We now describe the two approaches (nonlinear and weakly nonlinear theory) used to solve the flow problem.

A. Nonlinear theory

The nonlinear formulation is based on boundary integral equation methods for flow past a sluice gate [15,16] and a step in the bottom of a channel [8]. Some of the details are repeated for completeness, and further details can be found in these papers.

The dimensionless quantities $(x,y,\eta,\sigma,L,h) = (x^*,y^*,\eta^*,\sigma^*,L^*,h^*)/H$ and $(u,v) = (u^*,v^*)/U$ are defined by taking H as the reference length and U as the reference velocity. The free surfaces are then described by $y = 1 + \eta(x)$.

The nonlinear problem can be reduced to a problem in complex analysis. We first introduce the potential function ϕ and stream function ψ. We then define the complex potential, $f = \phi + i\psi$, and the complex velocity, $w = \frac{df}{dz} = u - iv$. Without loss of generality, we choose $\psi = 0$ on the streamline $ABCD$ with $\phi = 0$ $(x = 0)$ at point B. We denote by ϕ_c and x_c the values of ϕ and x at point C. It then follows that $\psi = -1$ on the bottom of the channel streamline $EFGH$. We denote the values of ϕ at the corners of the step by ϕ_f and ϕ_g $(x = x_h)$.

We define the function $\tau - i\theta$ as

$$w = u - iv = e^{\tau - i\theta}. \tag{4}$$

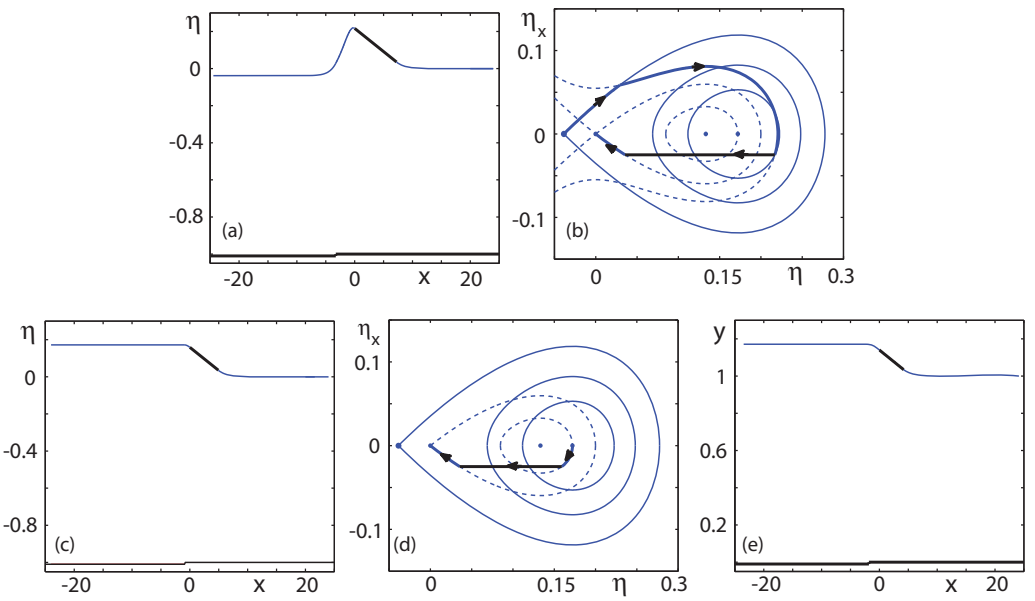

FIG. 2. (Color online) Flow with $F = 1.10$, $x_h < 0$, $h = -0.01$, and $\sigma_c = -0.025$. [(a) and (b)] Supercritical flow: Weakly nonlinear; $x_c = 7.25$, $x_h = -3.26$, $\eta_b = 0.22$, and $\eta_c = 0.04$. [(c)–(e)] Hydraulic fall: (c) and (d) Weakly nonlinear; $x_c = 4.94$, $x_h = -0.85$, $\eta_b = 0.16$, and $\eta_c = 0.04$. (e) Nonlinear; $x_c = 4.20$, $x_h = -1.81$, $\eta_b = 0.14$, and $\eta_c = 0.03$.

Following Binder *et al.* [16,26] (and others), we obtain the integral equation

$$\tau(\phi) = \frac{1}{2}\ln\frac{e^{\pi\phi_f}+e^{\pi\phi}}{e^{\pi\phi_g}+e^{\pi\phi}} - \frac{\phi_c}{\pi}\ln\frac{|e^{\pi\phi_c}-e^{\pi\phi}|}{|1-e^{\pi\phi}|} + \int_{-\infty}^{0}\frac{\theta(s)e^{\pi s}}{e^{\pi s}-e^{\pi\phi}}ds + \int_{\phi_c}^{\infty}\frac{\theta(s)e^{\pi s}}{e^{\pi s}-e^{\pi\phi}}ds, \quad (5)$$

which relates the values of τ and θ along $\psi = 0$.

On the free surfaces the dynamic boundary condition (3) becomes

$$e^{2\tau} + \frac{2}{F^2}y = 1 + \frac{2}{F^2}. \quad (6)$$

We relate the values of x and y on $\psi = 0$ by numerically integrating the identity

$$x_\phi + iy_\phi = \frac{1}{u - iv} = e^{-\tau+i\theta} \quad (7)$$

and equating real and imaginary parts. This gives a parametric representation $x = x(\phi)$, $y = y(\phi)$ for the streamline $\psi = 0$.

Two additional equations can also be obtained [8,16] for the sluice gate length, $L = (\eta_b - \eta_c)/\sin[\sigma_c]$, and step height, h. Equations (5)–(7), along with the equations for L and h, define a nonlinear integral equation for the unknown function $\theta(\phi)$ on the free surface. This integral equation is discretized, and the resulting algebraic equations are solved by Newton's method (see [8,15,16,26] for details).

B. Weakly nonlinear theory

The weakly nonlinear formulation combines the derivations for flow past a sluice gate [16] and step in the bottom of a channel [8]. Only the essentials are presented here.

The derivation is based on long wave asymptotics [4,5,8,16,26]. Thus if S denotes a typical horizontal length scale and H is the constant depth as $x^* \to \infty$, we introduce the small parameter $\epsilon = (H/S)^2 \ll 1$, the dimensionless spatial variables $(x', y') = (\epsilon^{1/2}x^*, y^*)/H$, and the free-surface elevation $\epsilon\eta' = \eta^*/H$. The dimensionless equation of the channel bottom is then $y' = \sigma'(x') = \epsilon^{-2}\sigma^*(x^*)/H$. The Froude number F is written as $F = 1 + \epsilon\mu$. Substituting expansions in powers of ϵ into the exact potential equations (rewritten in terms of the new scaled variables), a forced Korteweg–de Vries (KdV) equation is derived by equating coefficients of the successive powers of ϵ. This forced KdV equation (rewritten in terms of the variables $x = \epsilon^{-1/2}x', \eta = y - 1 = \epsilon\eta'$, and $\sigma = \epsilon^2\sigma'$ used in the nonlinear computations) is

$$\eta_{xx} + \tfrac{9}{2}\eta^2 - 6(F-1)\eta = -3\sigma. \quad (8)$$

We note that the forced KdV equation assumes that F is close to one and that waves are traveling only in one direction.

For $x > x_h$, $\sigma = 0$ and Eq. (8) then gives

$$\eta_{xx} + \tfrac{9}{2}\eta^2 - 6(F-1)\eta = 0. \quad (9)$$

The fixed points in the phase plane η_x versus η are at $\eta_x = 0$, $\eta = 0$, and $\eta = 4/3(F-1)$. For $F > 1$ there is a saddle point at $\eta = 0$, $\eta_x = 0$, and a center point at $\eta = 4/3(F-1)$, $\eta_x = 0$.

Integrating Eq. (9) yields

$$\eta_x^2 = 6(F-1)\eta^2 - 3\eta^3 + \bar{C}. \quad (10)$$

Here $\bar{C}$ is a constant of integration. This equation describes the free-surface downstream of the step.

For $x < x_h$, $\sigma = h$ and Eq. (8) then gives

$$\eta_{xx} + \tfrac{9}{2}\eta^2 - 6(F-1)\eta = -3h. \quad (11)$$

The fixed points are characterized by $\eta_x = 0$ and

$$\eta_1 = \frac{2}{3}(F-1) + \sqrt{\frac{4}{9}(F-1)^2 - \frac{2}{3}h} \quad \text{or}$$
$$\eta_2 = \frac{2}{3}(F-1) - \sqrt{\frac{4}{9}(F-1)^2 - \frac{2}{3}h}. \quad (12)$$

The fixed point labeled 2 is a saddle point. The fixed point labeled 1 is a center. Note that their existence requires $(F-1)^2 > 3h/2$. Integrating Eq. (11) yields

$$\eta_x^2 = 6(F-1)\eta^2 - 3\eta^3 - 6h\eta + \hat{C}. \quad (13)$$

Here $\hat{C}$ is a constant of integration. This equation describes the free surface upstream from the step.

Finally, the condition on the sluice gate is

$$\eta_x = -\tan[\sigma_c] \quad \text{on} \quad BC. \quad (14)$$

We note that the solutions of Eqs. (10) and (13) are not independent because the constants of integration $\bar{C}$ and $\hat{C}$ have to be determined so that the free surface is continuous.

III. RESULTS

The key idea now is to identify and classify qualitatively different types of solutions in the weakly nonlinear phase plane of the problem. For some of these types of solutions we then compute nonlinear solutions using the method described in Sec. II A. This is achieved by first plotting the two phase portraits using Eqs. (10) and (13) in the phase plane (η, η_x), for given values of F and h. In Fig. 2(b) the thin solid and broken curves correspond to the two phase portraits describing the free surface upstream of and downstream from the step, which we will shall refer to as $\tilde{A}$ and $\tilde{B}$, respectively. Solutions are then identified by considering the movements (due to the step and gate) between the trajectories and fixed points of the two phase portraits $\tilde{A}$ and $\tilde{B}$.

In Fig. 2(b) the movement due to the step in the phase plane is from the homoclinic orbit belonging to phase portrait $\tilde{A}$ (solid curves) onto the unbounded trajectory belonging to phase portrait $\tilde{B}$ (broken curves). The movement in the phase plane due to the gate is then from this unbounded trajectory along a horizontal line [see Eq. (14)] onto the homoclinic orbit belonging to phase portrait $\tilde{B}$. Shown in Fig. 2(a) is the weakly nonlinear free-surface profile in the physical plane (x, η) which corresponds to the phase plane diagram of Fig. 2(b).

Before continuing with the discussion of the results, we will comment on the general layout of Figs. 2–8. In each row of the figures (from left to right) there is a weakly nonlinear profile with its corresponding phase plane diagram. For some rows there is an additional computed fully nonlinear profile [see

Fig. 2(e)] in the physical plane (x,y), which can be compared with the weakly nonlinear results (in the same row).

A systematic approach is then taken in classifying the types of solution by first considering the two cases of when $h < 0$ and $h > 0$ in Secs. III A and III B, respectively, with $F > 1$. For both cases we present and discuss results as the position x_h of the step moves from left to right along the bottom of the channel. Then, in Sec. III C we consider solutions with $F = 1$ and $h < 0$.

A. A flow with $F > 1$ and $h < 0$

We begin the discussion of the results with the solution shown in the first row of Fig. 2. We classify this type of solution as supercritical flow, if there is waveless flow both far upstream of and downstream from the plate with $F^* > 1$ and $F > 1$.

The number of independent parameters for this type of solution can be determined by examining the phase plane diagram shown in Fig. 2(b). For example, given values of F and h provide the general layout of the two phase portraits (broken and thin solid curves), and a given value of σ_c determines the position of the horizontal line, in the phase plane. The journey through the phase plane begins at the saddle point moving in a clockwise direction along the homoclinic orbit of phase portrait $\tilde{A}$. The position x_h of the step on the bottom of the channel determines which unbounded trajectory of phase portrait $\tilde{B}$ we intersect with, and then continue to move along in the phase plane. The length of the plate L (or x_c and η_b) must then come as part of the solution. This ensures that the movement from the unbounded trajectory is onto the homoclinic orbit of phase portrait $\tilde{B}$. We then continue along the homoclinic orbit to the saddle point of phase portrait $\tilde{B}$. The number of independent parameters is then four, and they may be chosen as F, h, σ_c, and x_h.

For the type of solution illustrated in Figs. 2(a) and 2(b) there are two limiting cases to consider as the position of the step moves along the bottom of the channel (upstream of the gate). As the step's position moves upstream, the unbounded trajectory (of phase portrait $\tilde{B}$) approaches the trajectory that passes through the saddle point (0,0) in Fig. 2(b), and $x_h \to -\infty$. When the step's position moves downstream, the intersection of the homoclinic orbit (of phase portrait $\tilde{A}$) with the unbounded trajectory (of phase portrait $\tilde{B}$) moves in a clockwise direction around the homoclinic orbit (of phase portrait $\tilde{A}$). Ultimately, $x_h \to 0$ and the type of solution then becomes that shown in Figs. 3(a) and 3(b).

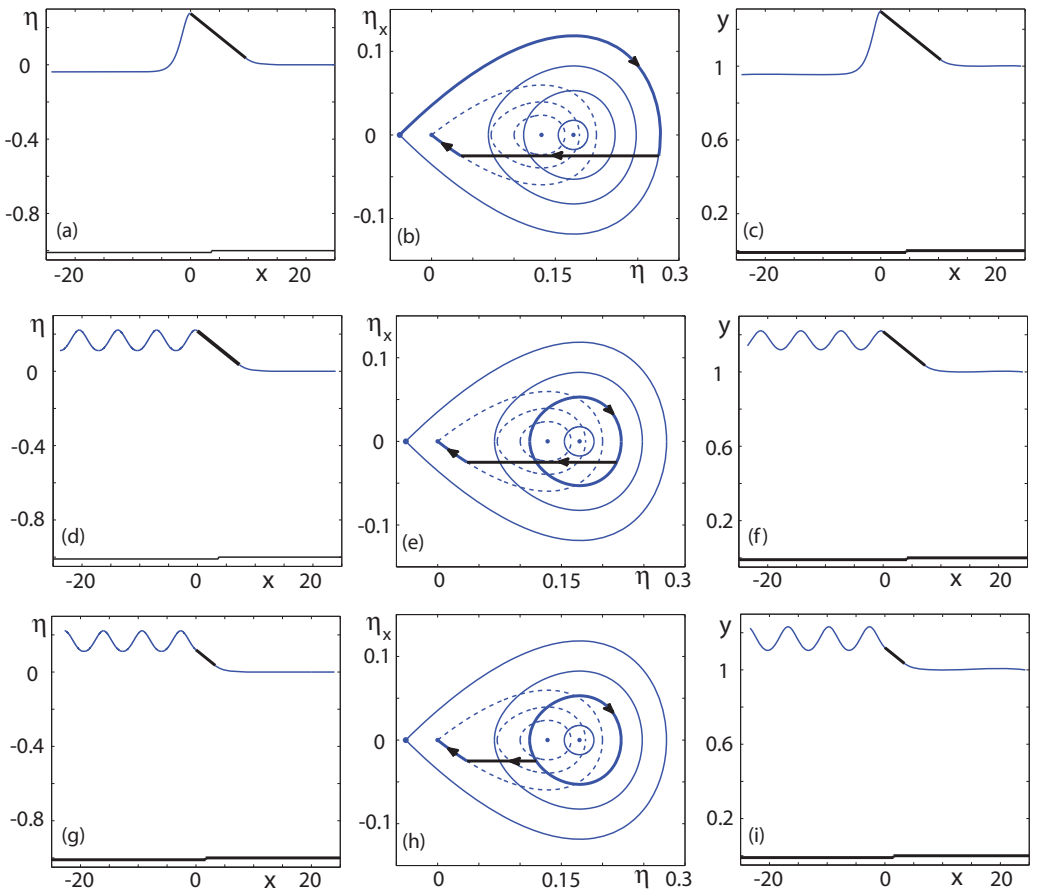

FIG. 3. (Color online) Flow with $F = 1.10$, $0 < x_h < x_c$, $h = -0.01$, and $\sigma_c = -0.025$. [(a)–(c)] Supercritical flow: (a) and (b) Weakly nonlinear; $x_c = 9.60$, $x_h = 3.63$, $\eta_b = 0.28$, and $\eta_c = 0.04$. (c) Nonlinear; $x_c = 10.34$, $x_h = 4.40$, $\eta_b = 0.30$, and $\eta_c = 0.04$. [(d)–(f)] Generalized critical flow: (d) and (e) Weakly nonlinear; $x_c = 7.26$, $x_h = 3.63$, $\eta_b = 0.22$, and $\eta_c = 0.04$. (f) Nonlinear; $x_c = 7.26$, $x_h = 4.11$, $\eta_b = 0.22$, and $\eta_c = 0.04$. [(g)–(i)] Generalized critical flow: (g) and (h) Weakly nonlinear: $x_c = 3.36$, $x_h = 1.68$, $\eta_b = 0.12$, and $\eta_c = 0.04$. (i) Nonlinear: $x_c = 3.39$, $x_h = 1.51$, $\eta_b = 0.12$, and $\eta_c = 0.03$.

Illustrated in the second row of Fig. 2 is a solution which we classify as a hydraulic fall, if there is waveless flow far upstream of and downstream from the plate with $F^* < 1$ and $F > 1$. The number of independent parameters for this type of solution is three, and they may be chosen as F, h, and σ_c. Here, the position x_h of the step and length of gate L must come as part of the solution to ensure the movement (due to step position) is from the center of phase portrait $\tilde{A}$ onto the inner periodic orbit of phase portrait $\tilde{B}$, and then from (due to length of gate) this periodic orbit onto the homoclinic orbit of phase portrait $\tilde{B}$.

As the position of the step moves upstream (for the type of solution shown in the second row of Fig. 2) there are additional solutions with an increasing number of waves trapped [25,27] between the step and gate. However, we choose not to present these solutions as they can be viewed as matchings of the already known solutions for generalized critical flow past a gate (see Fig. 6 in [16]) and subcritical flow past a step (see Fig. 6 in [8]). If we now fix the values of two extra parameters (e.g., x_h and L) there are also solutions with waves on the entire upstream free surface. This type of solution is now classified as generalized critical flow, if there is wavy subcritical flow far upstream and waveless supercritical flow far downstream. However, we also view these solutions as matchings of the already known solutions in [16] and [8], and so do not present them here.

In Fig. 3 we present results where the position of the step is underneath the sluice gate, i.e., within the interval $0 < x_h < x_c$. For all of the types of solution shown in Fig. 3, the movement between trajectories of the two phase portraits in the phase plane is solely due to the gate (along the horizontal lines in the phase plane diagrams of Figs. 3). In other words, the position of the step can be anywhere underneath the gate in the weakly nonlinear profiles. We also found there to be more or less no difference in the shape of the free surface as we varied the position of the step within the interval $0 < x_h < x_c$ in the corresponding nonlinear solutions.

The type of solution in the first row of Fig. 3 is supercritical flow. The independent parameters can be chosen as F, h, σ_c, and the choice of x_h (within $0 < x_h < x_c$) is arbitrary. The length of the plate L comes as part of the solution so that the movement in the phase plane [see Fig. 3(b)] is between the two homclinic orbits of the phase portraits $\tilde{A}$ and $\tilde{B}$.

Shown in the second and third rows of Fig. 3 are two types of qualitatively different solutions which can both be classified as generalized critical flow. They are obtained by fixing the value of an additional parameter (for example, L). The value of L then determines the periodic orbit of the phase portrait $\tilde{A}$ in the phase plane, or the amplitude of the waves on the upstream free surface.

As the length of the gate L increases to its maximum value, which is the value of L in the solution for supercritical flow, the waves on the upstream free surface approach their maximum amplitude—-the height of the perturbed solitary wave in Fig. 3(a). However, as L decreases, the amplitude of the waves first decreases to a minimum and then increases again. This minimum occurs when the length of the gate corresponds to the horizontal line intersecting with the periodic orbit (of the phase portrait $\tilde{A}$) directly below the center $(\eta_1,0)$ in the phase plane. For a flat gate the minimum of the wave amplitude is never zero, as it is impossible to intersect with the center in the phase plane. Hence, no solutions exist for hydraulic falls, when the position of the step is underneath the plate. This is similar to what was found [16] for flow just past a sluice gate.

So far we have seen that when the position of the step is upstream of the gate, we first move (due to the step) between the trajectories and fixed points of the two different phase portraits which is then followed by a movement (due to the gate) between the trajectories of phase portrait $\tilde{B}$, in the phase plane. When the position of the step is underneath the

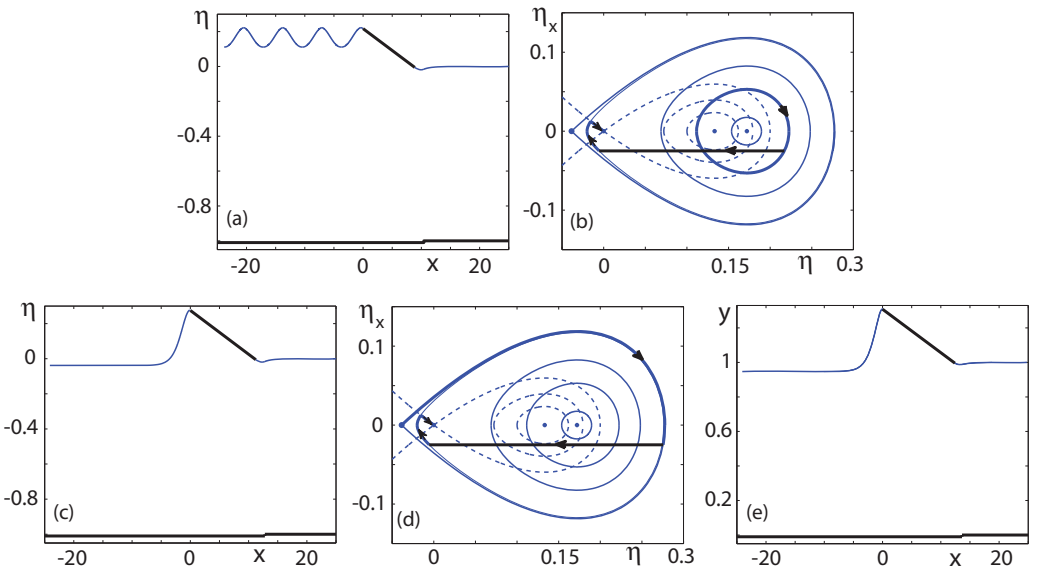

FIG. 4. (Color online) Flow with $F = 1.10$, $0 < x_c < x_h$, $h = -0.01$, and $\sigma_c = -0.025$. [(a) and-(b)] Generalized critical flow: Weakly nonlinear; $x_c = 8.88$, $x_h = 10.43$, $\eta_b = 0.22$, and $\eta_c = -0.01$. [(c)–(e)] Supercritical flow: (c) and (d) Weakly nonlinear; $x_c = 11.24$, $x_h = 12.79$, $\eta_b = 0.28$, and $\eta_c = -0.01$. (e) Nonlinear: $x_c = 12.41$, $x_h = 13.64$, $\eta_b = 0.31$, and $\eta_c = -0.01$.

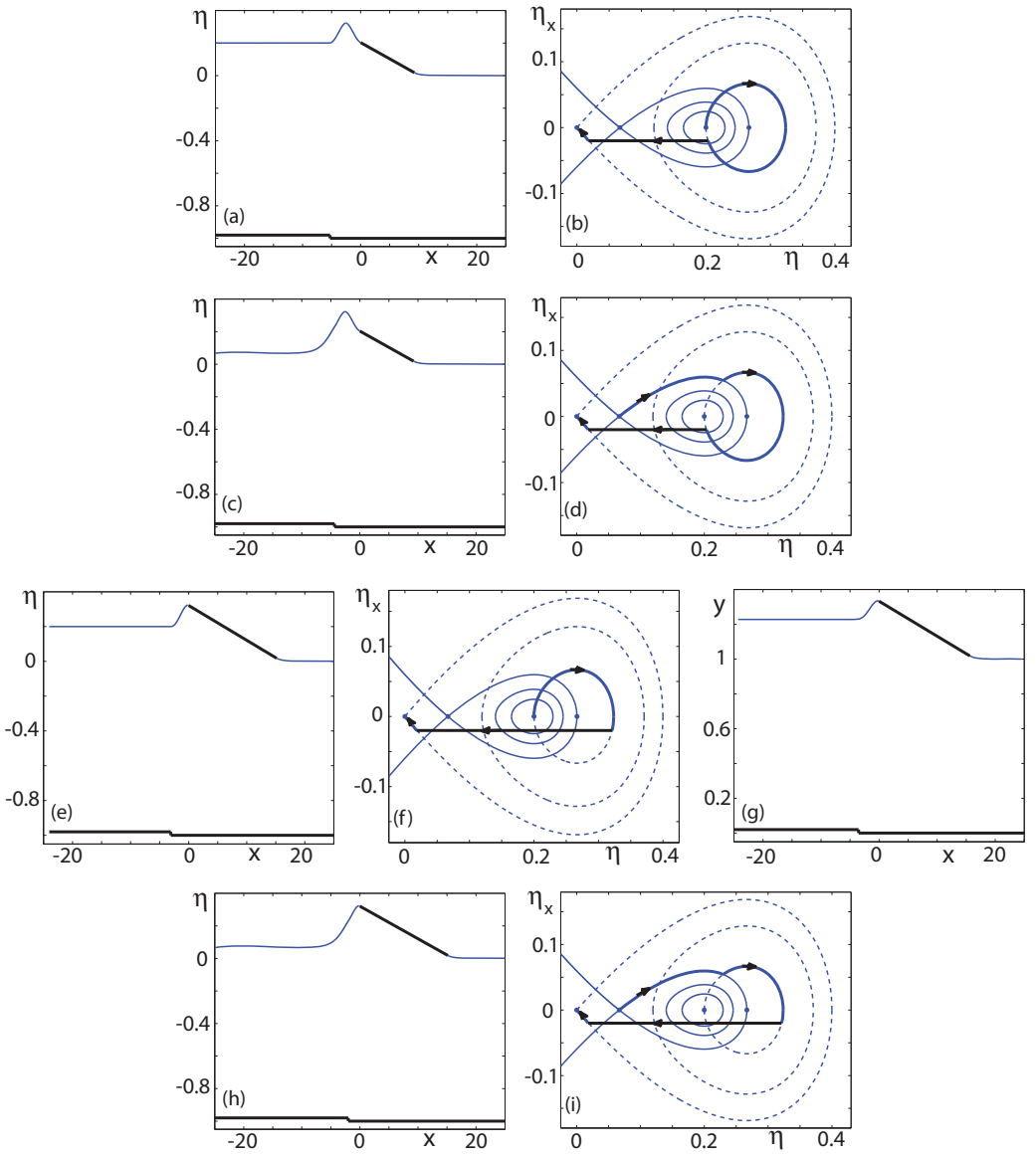

FIG. 5. (Color online) Flow with $F = 1.20$, $x_h < 0$, $h = 0.02$, and $\sigma_c = -0.02$. [(a) and-(b)] Hydraulic fall: Weakly nonlinear; $x_c = 9.27$, $x_h = -5.26$, $\eta_b = 0.20$, and $\eta_c = 0.02$. [(c) and (d)] Supercritical flow: Weakly nonlinear; $x_c = 9.27$, $x_h = -4.362$, $\eta_b = 0.20$, and $\eta_c = 0.02$. [(e)–(g)] Hydraulic fall: (e) and (f) Weakly nonlinear; $x_c = 15.16$, $x_h = -3.08$, $\eta_b = 0.32$, and $\eta_c = 0.02$. (g) Nonlinear; $x_c = 15.63$, $x_h = -3.53$, $\eta_b = 0.33$, and $\eta_c = 0.02$. [(h)and (i)] Supercritical flow: Weakly nonlinear; $x_c = 15.16$, $x_h = -2.00$, $\eta_b = 0.32$, and $\eta_c = 0.02$.

gate there is only one movement (due to the gate) which is between the trajectories of the two different phase portraits. We now discuss the results shown in Fig. 4, where the position of the step is downstream from the gate, i.e., $0 < x_c < x_h$. There are now two movements in the phase plane. The first (due to gate) is between the trajectories of phase portrait $\tilde{A}$, and the second (due to the step) is between the trajectories of the phase portraits $\tilde{A}$ and $\tilde{B}$. The number of independent parameters for a particular solution can be determined (in a similar way to that of Figs. 2 and 3) by analyzing phase plane diagrams.

Shown in the first and second rows of Fig. 4 are solutions for generalized critical flow and supercritical flow, respectively. For these two flow types there are several other qualitatively different looking solutions which we have not presented. However, there are no solutions for hydraulic falls when $0 < x_c < x_h$ (as it is impossible to intersect with the center of phase portrait $\tilde{A}$).

B. A flow with $F > 1$ and $h > 0$

We now turn our attention to investigating the qualitatively different types of solution for $F > 1, h > 0$, and $x_h < 0$. As the position of the step is upstream of the gate, the first movement is between the intersection of the fixed points and trajectories of phase portraits $\tilde{A}$ and $\tilde{B}$, followed by a second horizontal movement between the trajectories of phase portrait $\tilde{B}$ (see the phase plane diagrams of Fig. 5).

When examining just the profiles of Fig. 5 it is difficult to distinguish which solutions are hydraulic falls or supercritical flows. Demonstrated here, more than usual, is

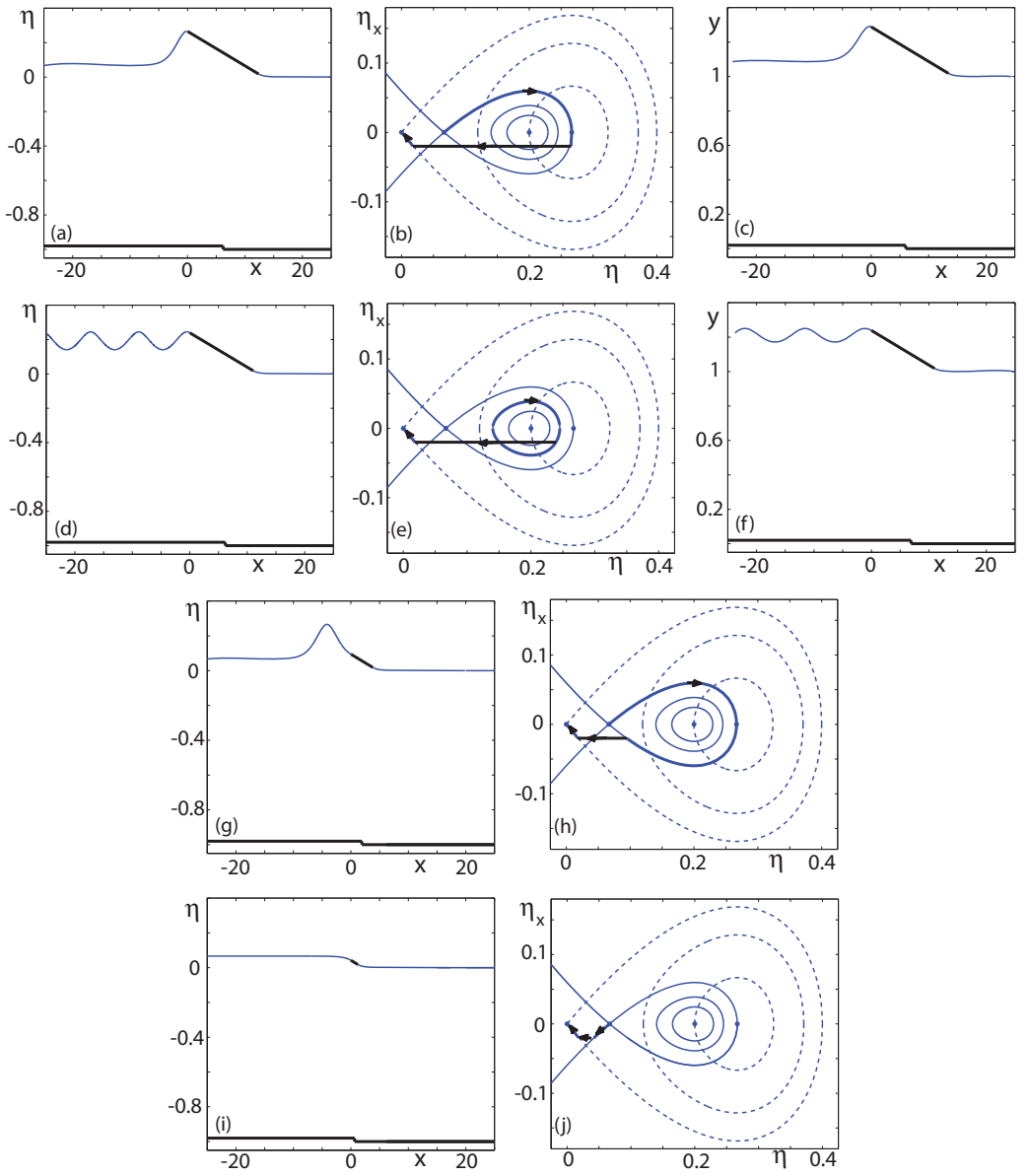

FIG. 6. (Color online) Flow with $F = 1.20$, $0 < x_h < x_c$, $h = 0.02$, and $\sigma_c = -0.02$. [(a)and (b)] Supercritical flow: Weakly nonlinear; $x_c = 12.38$, $x_h = 6.19$, $\eta_b = 0.27$, and $\eta_c = 0.02$. (c) Nonlinear; $x_c = 13.45$, $x_h = 6.01$, $\eta_b = 0.29$, and $\eta_c = 0.02$. [(d)–(f)] Generalized critical flow: (d) and (e) Weakly Nonlinear; $x_c = 11.06$, $x_h = 6.19$, $\eta_b = 0.24$, and $\eta_c = 0.02$. (f) Nonlinear; $x_c = 10.97$, $x_h = 6.89$, $\eta_b = 0.24$, and $\eta_c = 0.02$. [(g) and (h)] Supercritical flow: Weakly nonlinear; $x_c = 3.83$, $x_h = 1.92$, $\eta_b = 0.09$, and $\eta_c = 0.02$. [(i)and (j)] Supercritical flow: Weakly nonlinear; $x_c = 1.21$, $x_h = 0.65$, $\eta_b = 0.04$, and $\eta_c = 0.02$.

how the understanding of the corresponding phase plane diagrams assist in classifying the types of solutions. Solutions whose journeys in the phase plane begin with a center and end with a saddle are hydraulic falls, whereas those that begin with a saddle and end with a saddle are supercritical flows.

Shown in the first and third rows of Fig. 5 are two qualitatively different types of solutions which are hydraulic falls. They both look very different than the hydraulic fall shown in Fig. 2, where $h < 0$. Solutions with trapped waves on the upstream free surface and waves on the entire upstream free surface can also be obtained—these are then generalized critical flows. This is similar to what was discussed when $h < 0$ for the results in Fig. 2, and so we choose not to present these solutions in this paper.

Two qualitatively different types of solutions for supercritical flow are presented in the second and fourth rows of Fig. 5. Note that there was only *one* type of solution for supercritical flow when $h < 0$ (see Fig. 2).

When the position of the step is underneath the gate, we obtain the qualitatively different types of solutions shown in Fig. 6. The movement (due to the gate) in the phase plane is now solely between the trajectories of the two phase portraits $\tilde{A}$ and $\tilde{B}$, and the position of the step can be anywhere underneath the gate. This is similar to what we found when $h < 0$ (see Fig. 3). The solutions shown in the first, third, and fourth rows

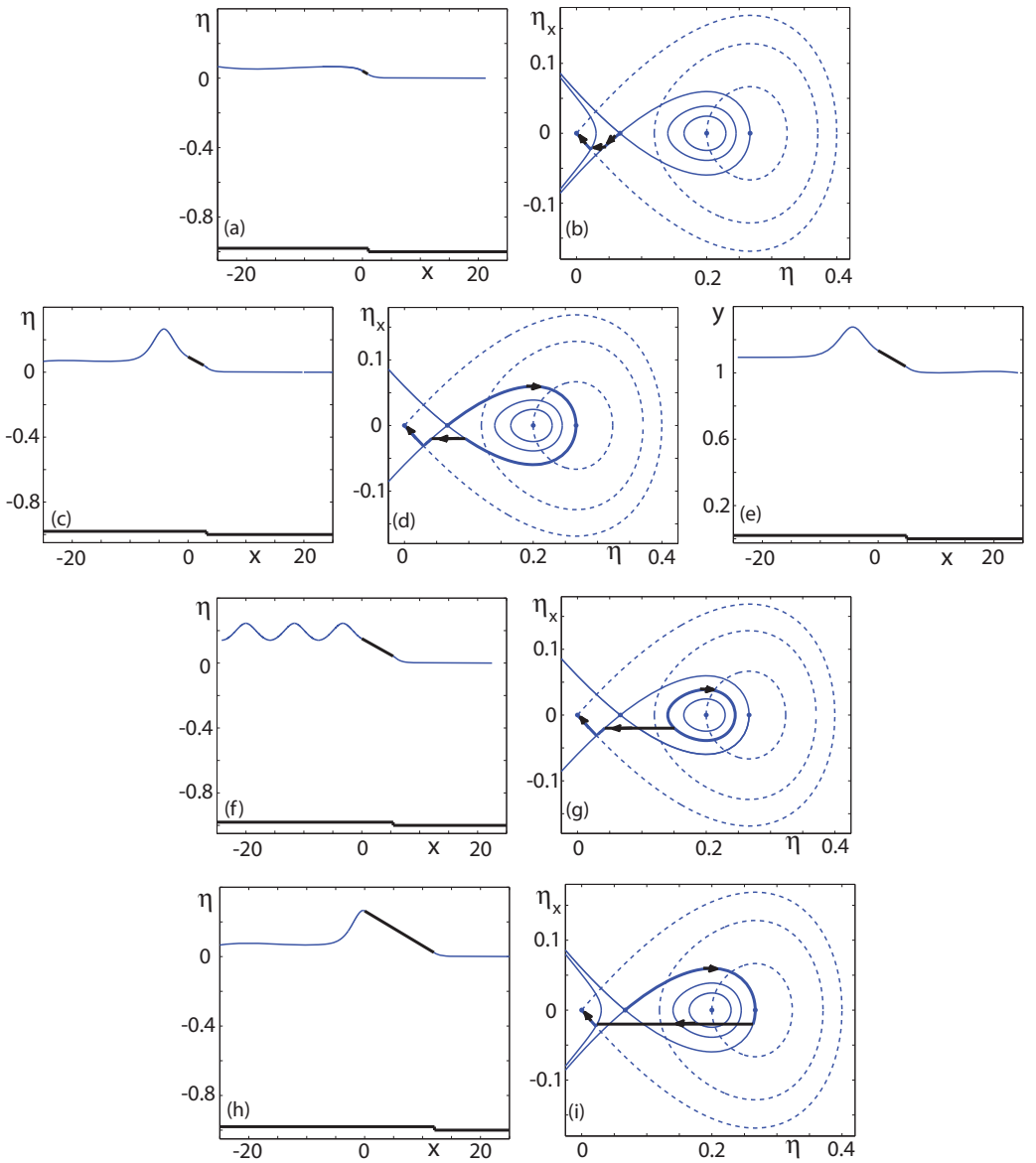

FIG. 7. (Color online) Flow with $F = 1.20$, $x_c < x_h$, $h = 0.02$, and $\sigma_c = -0.02$. [(a)and (b)] Supercritical flow: Weakly nonlinear; $x_c = 0.93$, $x_h = 1.02$, $\eta_b = 0.04$, adn $\eta_c = 0.02$. [(c)–(e)] Supercritical flow: (c) and (d) Weakly nonlinear; $x_c = 2.71$, $x_h = 3.21$, $\eta_b = 0.09$, and $\eta_c = 0.04$. (e) Nonlinear; $x_c = 4.72$, $x_h = 4.89$, $\eta_b = 0.13$, and $\eta_c = 0.04$. [(f)and (g)] Generalized critical flow: Weakly nonlinear; $x_c = 5.43$, $x_h = 5.93$, $\eta_b = 0.15$, and $\eta_c = 0.04$. [(h)and (i)] Supercritical flow: Weakly nonlinear; $x_c = 11.98$, $x_h = 12.06$, $\eta_b = 0.26$, and $\eta_c = 0.02$.

of Fig. 6 are supercritical flows, and the remaining solution shown in the second row of Fig. 6 is generalized critical flow.

In Fig. 7 we present qualitatively different types of solutions (with $h > 0$ and $F > 1$), where the position of the step is downstream from the gate. There are now two movements in phase plane, one due to each of the disturbances. The first movement is between the trajectories of phase portrait $\tilde{A}$ (gate) and the second is between the trajectories of the two phase portraits $\tilde{A}$ and $\tilde{B}$ (step). The solutions shown in the first, second, and fourth rows of Fig. 7 are supercritical flow, whereas the solution shown in the third row of Fig. 7 is generalized critical flow.

C. A flow with $F = 1$ and $h < 0$

Finally, we consider flows with $F = 1, h < 0$, and $x_c < x_h$. There are no solutions for flows with $F = 1$ when either $h > 0$ or $x_h < x_c$. In the phase plane the two fixed points belonging to the phase portrait $\tilde{B}$ have coalesced into a single fixed point at the origin (see the phase plane diagrams of Fig. 8).

These solutions are interesting enough in themselves, as we are unaware of any previously published results for steady flow past a gate with $F = 1$. On one hand they can be thought of as the continuous prolongation, as $F \to 1$ from above, of some of the solutions shown in Figs. 3 and 4. On the other hand, they can be viewed as the continuous prolongation, as $F \to 1$ from below, of solutions for subcritical flow (not considered

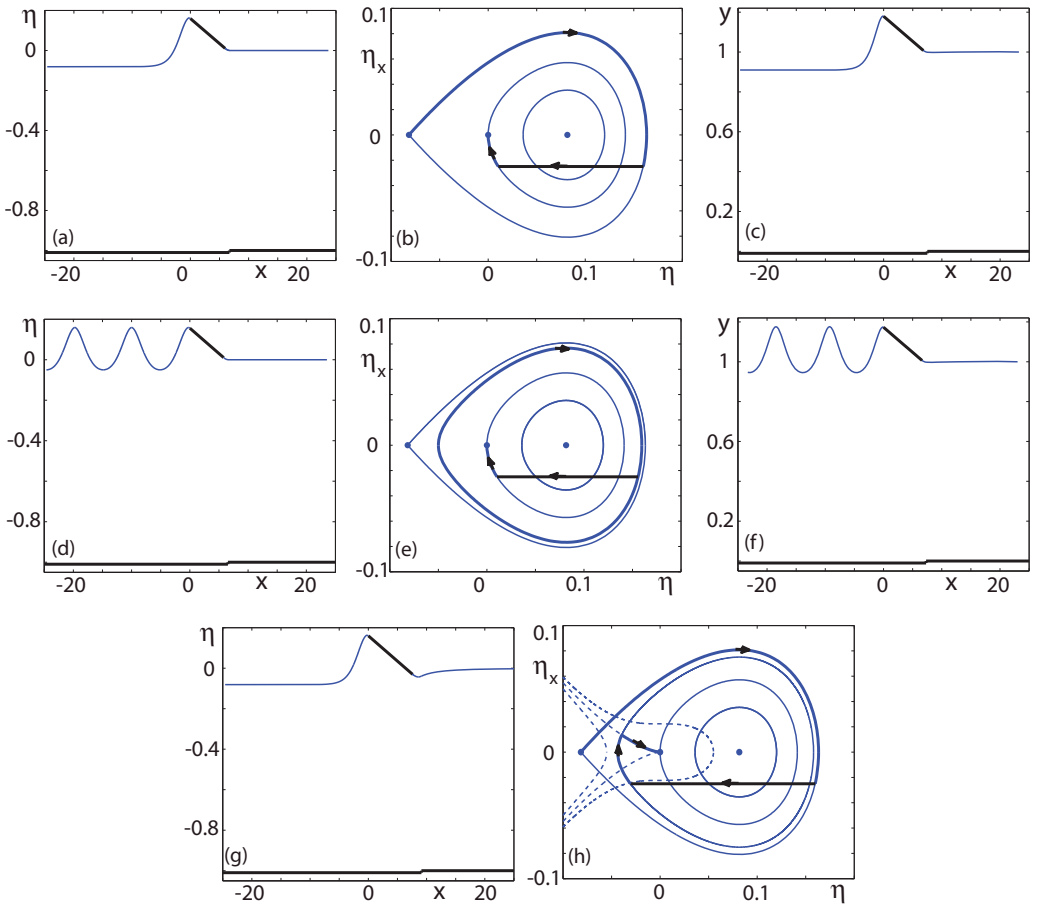

FIG. 8. (Color online) Flow with $F = 1.00$, $x_c < x_h$, $h = -0.01$, and $\sigma_c = -0.025$. [(a) and (b)] Weakly nonlinear; $x_c = 5.98$, $x_h = 6.71$, $\eta_b = 0.16$, and $\eta_c = 0.01$. (c) Nonlinear; $x_c = 6.84$, $x_h = 7.52$, $\eta_b = 0.18$, and $\eta_c = 0.01$. [(d) and (e)] Weakly nonlinear; $x_c = 5.81$, $x_h = 6.54$, $\eta_b = 0.16$, and $\eta_c = 0.01$. (f) Nonlinear; $x_c = 6.62$, $x_h = 7.31$, $\eta_b = 0.17$, and $\eta_c = 0.01$. [(g) and (h)] Weakly nonlinear; $x_c = 7.62$, $x_h = 9.12$, $\eta_b = 0.16$, and $\eta_c = -0.03$.

in this paper). In the latter case, there may then be a train of waves on the downstream free surface (when $F < 1$).

IV. CONCLUSION

Steady free-surface flows past a sluice gate and a step in the bottom of a channel have been investigated. A weakly nonlinear analysis of the phase space enabled us to systematically identify and classify many types of hybrid solutions. Nonlinear solutions were computed for some of these hybrids. Although we have restricted attention to flows when $F \geqslant 1$, a complementary study could be that for when $F \leqslant 1$. This would be of particular interest when investigating further the solutions for the case when $F = 1$.

[1] L.-K. Forbes, J. Eng. Math. **15**, 287 (1981).
[2] L.-K. Forbes, J. Eng. Math. **22**, 3 (1988).
[3] F. Dias and J.-M. Vanden-Broeck, J. Fluid Mech. **206**, 155 (1989).
[4] S. S-P. Shen, Q. Appl. Maths. **53**, 701 (1995).
[5] F. Dias and J.-M. Vanden-Broeck, J. Eng. Math. **42**, 291 (2002).
[6] A. C. King and M. I. G. Bloor, J. Fluid Mech. **182**, 193 (1987).
[7] S. S.-P. Shen and L. Gong, Phys. Fluids A **5**, 1071 (1993).
[8] B. J. Binder, F. Dias, and J.-M. Vanden-Broeck, Theor. Comput. Fluid Dyn. **20**, 124 (2006).
[9] B. J. Binder, J.-M. Vanden-Broeck, and F. Dias, IMA J. Appl. Math. **73**, 254 (2008).
[10] D. D. Frangmeier and T. S. Strelkoff, ASCE J. Engng Mech. Div. **94**, 153 (1968).
[11] B. E. Larock, ASCE J. Engng Mech. Div. **96**, 1211 (1969).
[12] Y. K. Chung, ASCE J. Engng Mech. Div. **98**, 121 (1972).
[13] N. Budden, Math. Proc. Cambridge Philos. Soc. **81**, 157 (1977).
[14] J.-M. Vanden-Broeck and J. B. Keller, J. Fluid Mech. **198**, 115 (1989).
[15] J.-M. Vanden-Broeck, J. Fluid Mech. **330**, 339 (1996).
[16] B. J. Binder and J.-M. Vanden-Broeck, Eur. J. Appl. Math. **16**, 601 (2005).
[17] B. J. Binder, F. Dias, and J.-M. Vanden-Broeck, J. Fluid Mech. **624**, 179 (2009).

[18] B. K. Ee, R. Grimshaw, D.-H. Zhang, and K. W. Chow, Phys. Fluids **22**, 056602 (2010).
[19] T. R. Akylas, J. Fluid Mech. **141**, 455 (1984).
[20] J. Asavanant, M. Paleewong, and Y. Choi, Commun. Korean Math. Soc. **16**, 137 (2001).
[21] J.-M. Vanden-Broeck, Eur. J. Appl. Math. **12**, 357 (2001).
[22] J.-M. Vanden-Broeck, *IUTAM Symposium on Diffraction and Scattering in Fluid Mechanics and Elasticity* (Kluwer Academic Publishers, Dordrecht, 2002), Vol. 41, p. 6168.
[23] E. Parau and J.-M. Vanden-Broeck, Eur. J. Mech. B/Fluids **21**, 643 (2002).
[24] R. Grimshaw, M. Maleewong, and J. Asavanant, Phys. Fluids **21**, 082101 (2009).
[25] F. Dias and J.-M. Vanden-Broeck, J. Fluid Mech. **509**, 93 (2004).
[26] B. J. Binder, J.-M. Vanden-Broeck, and F. Dias, Chaos **15**, 037106 (2005).
[27] B. J. Binder and J.-M. Vanden-Broeck, J. Fluid Mech. **576**, 475 (2007).
[28] L.-K. Forbes, J. Comput. Phys. **82**, 330 (1989).
[29] P. Mileswki and J.-M. Vanden-Broeck, Wave Motion **29**, 63 (1999).
[30] S. Grilli, P. Guyenne, and F. Dias, Int. J. Numer. Methods Fluids **35**, 829 (2001).
[31] E. Parau, J.-M. Vanden-Broeck, and M. J. Cooker, J. Fluid Mech. **538**, 99 (2005).
[32] F. Dias and T. J. Bridges, Fluid Dyn. Res. **38**, 830 (2006).